

文章编号: 1006-9941 (2015)12-1217-04

# Flowability and Infrared Interference Properties of Modified Graphite Flake with Hydrophobic Nano-silica

NING Gong-tao<sup>1</sup>, LI Ping<sup>1</sup>, CUI Yu-ling<sup>2</sup>, LI Shi-chuan<sup>3</sup>, TANG Run-ze<sup>3</sup>, ZHOU Zun-ning<sup>3</sup>

(1. National Key Laboratory of Mechatronic Engineering and Control, Beijing Institute of Technology, Beijing 100081, China; 2. 73921 Troops, Nanjing 210016, China; 3. State Key Laboratory of Explosion Science and Technology, Beijing Institute of Technology, Beijing 100081, China)

**Abstract:** To research the dispersion properties and infrared (IR) interference efficiency of graphite flake particulates modified by hydrophobic nano-silica, the flowability of graphite flake particles before and after modification was measured by a powder property tester. The smoke was formed by dispersing the graphite flake particles into the smoke box using air flow dispersion way. The mass concentration and IR spectrum transmission of the smoke were measured. On the basis of stir settlement model, the settling velocity of smoke was calculated. Results show that the Carr's flowability index of graphite flake particulates modified with hydrophobic nano-silica in mass ratio of 4.0 % is the highest, reaching 61 and at the same time, the settling velocity decreases from  $2.288 \times 10^{-3} \text{ m} \cdot \text{s}^{-1}$  before modification to  $1.125 \times 10^{-3} \text{ m} \cdot \text{s}^{-1}$  after modification. Average IR spectrum transmission of the smoke formed in the wave band range of 3–5  $\mu\text{m}$  and 8–12  $\mu\text{m}$  decreases from 0.3895 % and 0.7288 % to 0.072 % and 0.176 %. The physical modification of hydrophobic nano-SiO<sub>2</sub> on graphite flake surface effectively improves the flowability and dispersion properties and significantly increases the duration of the smoke formed by graphite flake particles and IR interference performance.

**Key words:** electro-optical countermeasure; graphite flake; hydrophobic nano-SiO<sub>2</sub>; obscurants; flowability

**CLC number:** TJ55

**Document code:** A

**DOI:** 10.11943/j.issn.1006-9941.2015.12.013

## 1 Introduction

The advent of more advanced infrared (IR) sensors containing sophisticated target acquisition and guidance systems spurred the development of smokes that attenuate light in the IR wavelengths<sup>[1-2]</sup>. A variety of offensive and defensive systems and materials are employed on the battlefield. The most popular IR smokes are solid materials of graphite flakes that have good IR absorption properties because of their moderately strong molecular vibrations in the IR region<sup>[3-4]</sup>.

Graphite flake material must be disseminated and airborne to be effective as an electromagnetic obscurant. The graphite flake aerosols are mechanically generated using compressed-air systems. The powder is directly delivered to the air-ejector of smoke generators. The demand for effective graphite flake aerosols formulation is increased for better delivery efficiency and dispersion capability. The flowability of graphite flake particles is particularly important because it influences the delivery process and dissemination efficiency. However, most studies are focused on graphite flake particles with various sizes to improve the IR extinction performance<sup>[5-6]</sup>. Graphite flakes used for IR smokes are very easy to be combined with atmospheric water because of having a greater specific surface area and smaller particle size. If graphite flakes are coated by water or formed agglomerates between graphite flake particles, their settling velocity will be accelerated and infrared extinction performance will be degraded<sup>[7-8]</sup>.

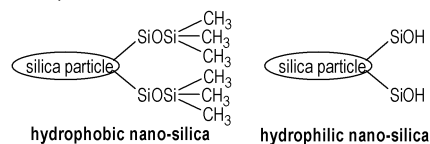
Most literatures have shown that hydrophobic nano-particles may modify powders and improve the flowability between

powder particles<sup>[5, 7-10]</sup>. The research presented in this paper focuses on the evaluation of the flowability and extinction performance of modified graphite flakes with hydrophobic nano-silica. The index of flowability and IR spectrum transmittance of surface modification of graphite flakes were determined and compared with those of unmodified graphite flake particles.

## 2 Experimental

### 2.1 Materials

Hydrophobic nano-silica (AEROSIL R202) powder was chosen as guest particles supplied by German Evonik Degussa. The nano-silica has highly hydrophobic characteristic because its —SiOSi(CH<sub>3</sub>)<sub>3</sub> groups (Scheme 1). As shown in Scheme 1, silica particle with lots of —SiOH groups is sensitive to the variations of humidity. The median particle size of hydrophobic nano-silica,  $D_{50}$  is about 15 nm. This material is a fine, white, cohesive and hydrophobic powder widely used in medicine and catalyst, etc.



Scheme 1

Graphite is a soft-scale form of carbon that can be natural or synthetic in origin. Natural graphite was provided by Chinese Qingdao OER graphite Co. LTD and chosen as host particles. The chemical composition of the bulk powder is predominantly carbon with trace impurities totaling less 1% by mass. The trace impurities include small quantities of silica, aluminum, iron, calcium, titanium, and magnesium. Fig. 1 shows a TEM picture of nature graphite particles. Their surface seems to have fish scale-like form.  $D_{50}$  is about 6  $\mu\text{m}$ .

**Received Date:** 2015-02-08; **Revised Date:** 2015-03-31

**Project Supported:** National Defense Key Projects (1011)

**Biography:** NING Gong-tao (1974–), male, doctor, majoring in electro-optical materials

**Corresponding Author:** ZHOU Zun-ning (1969–), male, associate professor, majoring in electro-optical countermeasure. e-mail: zzn@bit.edu.cn

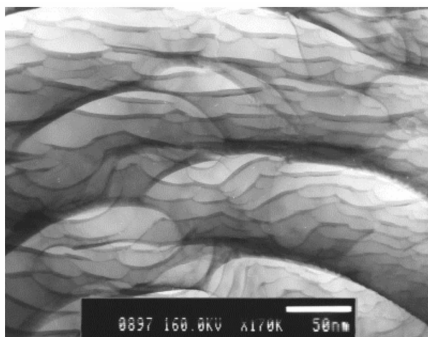


Fig. 1 TEM image of nature graphite flake

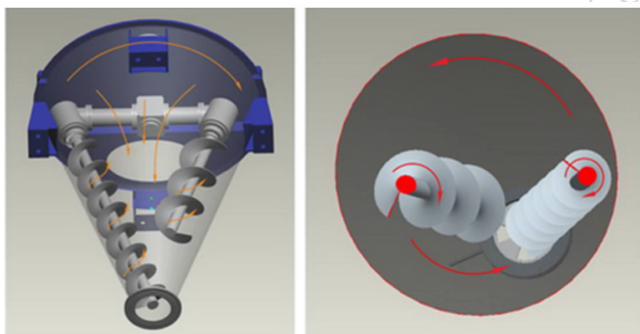


Fig. 2 Model DSH-0.5 double screw conical mixer

## 2.2 Modifying Processes

A double screw conical mixer (Model DSH-0.5) was chosen to perform a dry coating in this study. This apparatus was defined as a high shear mixer, manufactured by Shanghai Shen-li machinery Co. Ltd, China. As it can be seen from Fig. 2, it rotated around its axes by right of two internal asymmetric spirals which was installed on the cantilever. Mean while, the rotational force from the cantilever drove two spiral doing revolution around conical chamber axle wire. It applied high mechanical impact and shearing forces on the particles in order to break the fine agglomerates and coated them on the host particles. This way could full the bottom gap and form a convective circulation. The dry coating method was also used successfully for dry particle coating experiment<sup>[9-11]</sup>. The operating condition was  $1500 \text{ r} \cdot \text{min}^{-1}$  for 40 min at room temperature.

## 2.3 Characterization

The various characterization methods were used after dry particle coating. The surface morphology of the particles was observed by scanning electron microscopy (Hitachi Model S-4800). The powder tester (TC-1000/1001) was used to examine the flowability of the unmodified and modified samples. The  $20 \text{ m}^3$  ( $6.1 \text{ m} \times 2.0 \text{ m} \times 1.8 \text{ m}$ ) smoke chamber used to measure the performance parameters such as IR spectrum transmittance of aerosol, settling velocity, mass concentration was shown in Fig. 3 with the full smoke characterization instrument configuration. Glass fiber filters, a rotometer and vacuum pump were used to make aerosol concentration measurements at a flow rate of 36 liters per minute. The aerosol transmittance over the wavelength range of  $1.34\text{--}13.94 \mu\text{m}$  was measured by an IR spectrometer (Model 12-550 Mark III, USA) with HgCdTe

detector operated at liquid nitrogen temperature.

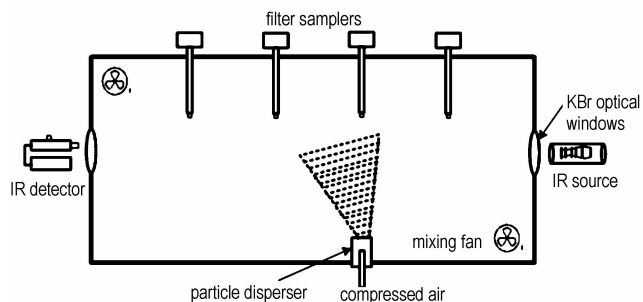


Fig. 3 Schematic diagram of the particles chamber showing the instruments

A known mass (approximately 30 g) of particles was placed inside the powder disperser, which was connected to a compressed air tank through a hose and nozzle. The nozzle was operated at 202.6 MPa to disperse and deaggregate powders to produce an aerosol of primary particles. Two mixing fans were operated continuously in the chamber at a low speed to maintain uniform concentration and provided a level of turbulence driving re-aerosolization and impaction approximating those components of aerosol deposition in the battlefield. Spectral scans started to record data after finished powder dissemination, at the same time, the aerosol mass concentration measurement was started. Repeated measurements were made by stopping 1 min after finished particles sampling.

## 3 Results and Discussion

### 3.1 The Flow Property of Graphite Flake Particles

The flow property of particles is a very important factor in the process of powder handling such as storage, portage and transfer. The phrase “good flow behaviour” usually means that a bulk solid flows easily, i. e., it does not consolidate much and flows out of a silo or a hopper due to the force of gravity alone, and no flow promoting devices are required. Products are “poorly flowing” if they experience flow obstructions or consolidate during storage or transport. Carr<sup>[12]</sup> suggested a method for evaluating the flowability from his experience on the handling of various powders. The flowability ( $F_w$ ) was calculated using the sum of indices suggested by Carr for the angle of repose ( $\theta_r$ ), angle of spatula ( $\theta_s$ ), degree of uniform ( $U_i$ ) and compressibility ( $C_p$ ).  $F_{wz}$  is a common way to characterize the flow behavior of particles. Higher  $F_{wz}$  values indicate better flowability. The flowability index can be calculated by Eq. (1):

$$F_{wz} = \theta_{rz} + \theta_{sz} + C_{pz} + U_{iz} \quad (1)$$

where  $F_{wz}$  is the flowability index;  $\theta_{rz}$  is the angle of repose index;  $\theta_{sz}$  the angle of spatula index;  $C_{pz}$  is the compressibility index and  $U_{iz}$  is the degree of uniform index.

Table 1 summarizes the values of the flowability index of the unmodified and modified graphite flake calculated using the angle of repose index, angle of spatula index and compressibility index according to powder evaluation method suggested by Carr. The angle of repose and compressibility of the modified graphite flake gradually reduce with increasing in the mass of nano-SiO<sub>2</sub>, indicating an agglomeration decreases between

**Table 1** Flowability of the unmodified and modified graphite flake

mass of nano-silica /%	$\theta_r / (^\circ)$	$\theta_{rz}$	$\theta_s / (^\circ)$	$\theta_{sz}$	$C_p / \%$	$C_{pz}$	$U_f$	$U_{fz}$	$F_{wz}$
0	46.0	14.5	77.0	7	44.0	2.0	2.24	23	46.5
1	45.7	15.0	71.5	12	42.7	2.0	2.24	23	52.0
2	45.7	15.0	70.8	12	36.7	5.0	2.24	23	55.0
3	44.3	16.0	68.0	12	36.0	7.0	2.24	23	58.0
4	43.7	16.0	69.3	12	30.7	10.0	2.24	23	61.0
5	46.0	14.5	74.7	10	32.0	9.5	2.24	23	57.0

the graphite flake particles. When the nano-silica mass ratio is 4.0%, the value of  $\theta_r$  reaches the minimum and  $F_{wz}$  becomes maximum. This means that the flowability is improved through surface treatment.

### 3.2 Graphite Flakes Aerosol Properties

Each value of mass concentration represents the mean of four different sampling locations (see Table 2). In order to ob-

tain the settling velocity, the following equation is employed based on a series of two filter concentration measurements<sup>[13]</sup>

$$v_d = \frac{H}{t_2 - t_1} \ln \frac{C(t_1)}{C(t_2)} \quad (2)$$

where  $v_d$  is the settling velocity in  $m \cdot s^{-1}$ ,  $H$  is the chamber height in m,  $C(t_1)$  is the mass concentration taken over time intervals  $t_1$  to  $(t_1+1)$ , in  $g \cdot m^{-3}$  and  $C(t_2)$  is the mass concentration taken over time intervals  $t_2$  to  $(t_2+1)$  in  $g \cdot m^{-3}$ .

**Table 2** Mass concentration and settling velocity of particles in chamber

mass fraction of nano-silica /%	mass concentration at different time intervals/ $g \cdot m^{-3}$				average mass concentration at different time intervals/ $g \cdot m^{-3}$
	0-1 min	2-3 min	4-5 min	6-7 min	
0	1.1319	0.8156	0.6325	0.5125	2.288
1	1.0944	0.8256	0.6513	0.5356	2.134
2	1.1306	0.9431	0.7906	0.6600	1.587
3	1.0762	0.8925	0.7638	0.6538	1.401
4	1.1281	0.9363	0.8263	0.7131	1.125
5	1.0562	0.8531	0.6681	0.5831	2.200

The IR spectrum radiance values measured by the Mark III spectrometer are converted to transmittance ( $T(\lambda)$  values using Eq. (3).

$$T(\lambda) = \frac{L'_t(\lambda) - L_{bs}(\lambda)}{L'_t(\lambda) - L_{bak}(\lambda)} \times 100\% \quad (3)$$

where  $L'_t(\lambda)$  is the target spectrum radiance without the obscurant in  $W/Sr \cdot m^2 \cdot \mu m$ ,  $L_{bak}(\lambda)$  is the background spectrum radiance without the obscurant and the blackbody in  $W/Sr \cdot m^2 \cdot \mu m$ ,  $L'_t(\lambda)$  is the target spectrum radiance with the obscurant in  $W/Sr \cdot m^2 \cdot \mu m$  and  $L_{bs}(\lambda)$  is the spectrum radiance of the obscurant and background without the blackbody in  $W/Sr \cdot m^2 \cdot \mu m$ .

The values of the band-averaged transmittance of unmodified and modified graphite flake aerosols are calculated using Eq. (4).

$$\bar{T} = \int_{\lambda_1}^{\lambda_2} \frac{T(\lambda) d\lambda}{\lambda_2 - \lambda_1} \times 100\% \quad (4)$$

Table 3 summarizes the values of the band-averaged transmittance of unmodified and modified graphite flake aerosols.

The data of band-averaged transmittance of particles in Table 3 gradually decrease with increasing the mass of nano-silica. Fig. 4 shows the IR spectrum transmittance of unmodified and modified graphite flake with the nano-SiO<sub>2</sub> mass ratio of 4.0% at 4-5 min. The mean transmittance value of modified graphite flake is 0.072% in the range of 3-5  $\mu m$  and 0.176% in the range of 8-14  $\mu m$ , which is significantly different from 0.3895% in the range of 3-5  $\mu m$  and 0.7288% in the range of 8-12  $\mu m$  of unmodified graphite flake. Many factors can influence the IR extinction properties of obscurants, including the conductivity, air concentration, and morphology, etc<sup>[14]</sup>.

**Table 3** Band-averaged transmittance of graphite flake aerosols in particles chamber

mass fraction of nano-silica /%	wavelength / $\mu m$	averaged transmittance at different time intervals/%			
		0-1 min	2-3 min	4-5 min	6-7 min
0	3-5	0.0464	0.1896	0.3895	0.7922
	8-14	0.0716	0.2221	0.7288	0.8904
1	3-5	0.0320	0.1462	0.2002	0.5365
	8-14	0.1338	0.2193	0.4017	0.7047
2	3-5	0.0295	0.0567	0.1880	0.3230
	8-14	0.0176	0.1126	0.3643	0.6663
3	3-5	0.0087	0.0645	0.1825	0.2837
	8-14	0.0207	0.0990	0.2442	0.5682
4	3-5	0.0104	0.0440	0.0720	0.1680
	8-14	0.0083	0.0751	0.1760	0.3098
5	3-5	0.0374	0.1090	0.3952	0.9896
	8-14	0.1542	0.3654	0.9084	0.9163

Morphology is particularly important because it influences the coagulation process and removal of particles from the air<sup>[15-16]</sup>. The surface morphology of modified graphite flake with nano-silica in Fig. 5b is smoother than unmodified graphite flake in Fig. 5a. That can help the particles to have better flowability. This change minimizes the coagulation between the graphite flake particles and lowers the settling velocity of particles when larger clusters of graphite flake particulates can not be formed. The settling velocity decreases from  $2.288 \times 10^{-3} m \cdot s^{-1}$  of unmodified graphite flake to  $1.125 \times 10^{-3} m \cdot s^{-1}$  of modified graphite flake (see Table 2). However, after this optimal amount of

nano-silica, the settling velocity increases. The reason for this increase is unclear and further studies are needed in order to clarify the mechanism behind.

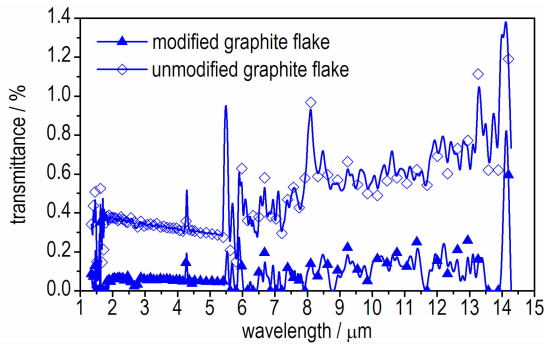


Fig. 4 IR spectra transmittances of unmodified and modified graphite flake particles at 4–5 min

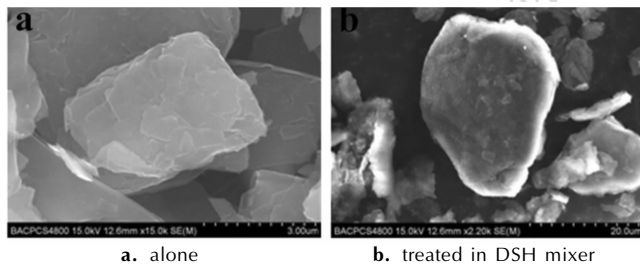


Fig. 5 SEM (Model S-4800) images of graphite flake treated with silica

#### 4 Conclusions

(1) A method of modifying the graphite flake particle surface with hydrophobic nano-SiO<sub>2</sub> using the dry particle coating process is presented.

(2) The Carr's flowability index of graphite flake particulates modified with hydrophobic nano-silica in mass ratio of 4.0% is the highest, reaching 61.

(3) This physical modification makes the settling velocity of modified graphite flake decrease from  $2.288 \times 10^{-3} \text{ m} \cdot \text{s}^{-1}$  before modification to  $1.125 \times 10^{-3} \text{ m} \cdot \text{s}^{-1}$  after modification and the duration of graphite flake particles floating in air increases.

**Acknowledgement:** The authors are grateful to the State Key Laboratory of Explosion Science and Technology (Beijing Institute of Technology) for experimental support of projects.

### 疏水纳米 SiO<sub>2</sub> 改性鳞片石墨的流动性及红外干扰性能

宁功韬<sup>1</sup>, 栗苹<sup>1</sup>, 崔玉玲<sup>2</sup>, 李石川<sup>3</sup>, 汤润泽<sup>3</sup>, 周遵宁<sup>3</sup>

(1. 北京理工大学机电控制工程国防重点实验室, 北京 100081; 2. 73921 部队, 江苏 南京 210016; 3. 北京理工大学爆炸科学与技术国家重点实验室, 北京 100081)

**摘要:** 为研究疏水纳米 SiO<sub>2</sub> 改性鳞片石墨的分散性能和红外干扰效能, 采用粉体特性测试仪测定了改性前后鳞片石墨粒子的流动性。采用气流分散的方式将鳞片石墨粒子分散在烟幕箱中形成烟幕。测试了烟幕的质量浓度和红外光谱透过率。依据搅拌沉降模型, 计算得到了烟幕的沉降速度。结果表明, 用质量分数为 4.0% 的疏水纳米 SiO<sub>2</sub> 改性鳞片石墨的 Carr 流动性指数最高, 达到了 61, 同时鳞片石墨粒子的沉降速度也从改性前的  $2.288 \times 10^{-3} \text{ m} \cdot \text{s}^{-1}$  降至改性后的  $1.125 \times 10^{-3} \text{ m} \cdot \text{s}^{-1}$ , 形成的烟幕在 3~5 μm 和 8~12 μm 波段的平均红外光谱透过率也分别从 0.3895% 和 0.7288% 降为 0.072% 和 0.176%。疏水纳米 SiO<sub>2</sub> 对鳞片石墨表面的物理修饰, 有效改善了鳞片石墨粒子的流动性和分散性能, 显著提高了鳞片石墨形成烟幕的留空持续时间和红外干扰性能。

**关键词:** 光电对抗; 鳞片石墨; 疏水纳米 SiO<sub>2</sub>; 遮蔽; 流动性

中图分类号: TJ55

文献标识码: A

DOI: 10.11943/j.issn.1006-9941.2015.12.013

#### References:

- [1] Albertoni A. Long wave infrared metamaterials and nano-materials design, simulation and laboratory test for target camouflage in the defence application [C] // Proc of Electro-Optical and Infrared Systems: Technology and Applications VIII. Prague: SPIE, 2011, 8185: 1–19.
- [2] Viau C R. Expendable countermeasure effectiveness against imaging infrared guided threats [R]. Tactical Technologies Inc, 2012
- [3] Mukhopadhyay P, Gupta R K. Graphite, graphene and their polymer nanocomposites [M]. New York: CRC press, 2013: 1–10.
- [4] Petrov M B. Modeling of magnetoelectric effects in composites [M]. New York: Springer, 2014: 10–33.
- [5] Pjesky S C, Maghirang R G. Infrared extinction properties of nanostructured and conventional particles [J]. *Particulate Science and Technology*, 2012, 30(2): 103–118.
- [6] Yadav A, Kumar R, Bhatia G, et al. Development of mesophase pitch derived high thermal conductivity graphite foam using a template method [J]. *Carbon*, 2011, 49(11): 3622–3630.
- [7] Focke W F, Badenhorst H, Ramjee S, et al. Graphite foam from pitch and expandable graphite [J]. *Carbon*, 2014, 73: 41–50.
- [8] CHEN Zong-sheng, SHI Jia-ming, YUAN Zhong-cai, et al. Effect of wrapped liquid on IR extinction characteristics of graphite spheres [J]. *The Chinese Journal of Infrared*, 2007, 28(12): 30–33.
- [9] CHIU Chih-cheng, LO Jen-chieh, TENG Mao-hua. A novel high efficiency method for the synthesis of graphite encapsulated metal (GEM) nanoparticles [J]. *Diamond & Related Materials*, 2012, 24: 179–183.
- [10] Akira S, Eric S, Philippe G, et al. Experiment and simulation of dry particle coating [R]. Granulation Conference Lausanne, Switzerland, 2011.
- [11] Ouabbas Y, Dodds J, Galet L, et al. Particle-particle coating in a cyclomix impact mixer [J]. *Powder Technology*, 2009, 189(2): 245–252.
- [12] Honda H, Kimura M, Honda F, et al. Preparation of monolayer particle modified powder by the dry impact blending process utilizing mechanochemical treatment [J]. *Colloids and Surfaces A: Physicochemical and Engineering Aspects*, 1994, 82(2): 117–128.
- [13] Carr R L. Classifying flow properties of solids [J]. *Chemical Engineering*, 1965, 72: 69–72.
- [14] Embury J F, Walker D L, Zimmermann C J. Screening smoke performance of commercially available powders I. Infrared screening by graphite flake [R]. No: ERDEC-TR-093, Edgewood Research Development & Engineering Center, Edgewood, MD, USA, 1993.
- [15] Appleyard P G, Davies N. Modeling infrared extinction of high aspect ratio, highly conducting small particles [J]. *Journal of Optics A*, 2004, 6(10): 977–990.
- [16] Bohren C F, Huffman D R. Scattering, absorption, and emission of light by small particles [M]. New York: Cambridge University Press, 2002: 68–82.